

## RAPID COMMUNICATION

# Dynamic stability threshold in high-performance internal-tin Nb<sub>3</sub>Sn superconductors for high field magnets

A K Ghosh<sup>1</sup>, E A Sperry<sup>1</sup>, L D Cooley<sup>2</sup>, A M Moodenbaugh<sup>2</sup>,  
R L Sabatini<sup>2</sup> and J L Wright<sup>2</sup>

<sup>1</sup> Superconducting Magnet Division, Brookhaven National Laboratory, Upton, NY 11973, USA

<sup>2</sup> Materials Science Department, Brookhaven National Laboratory, Upton, NY 11973, USA

E-mail: aghosh@bnl.gov

Received 24 September 2004, in final form 5 November 2004

Published 1 December 2004

Online at [stacks.iop.org/SUST/18/L5](http://stacks.iop.org/SUST/18/L5)

## Abstract

Modern Nb<sub>3</sub>Sn strands can now exceed 3000 A mm<sup>-2</sup> critical current density  $J_c$  at 4.2 K and 12 T within the non-copper area. However, the aggressive reaction used to achieve this performance causes the Nb<sub>3</sub>Sn filaments to coalesce into a single large, continuous ring of superconductor, and also allows tin to penetrate through diffusion barriers and alloy with the copper stabilizer. This results in a lack of adiabatic stability, due to the combination of high  $J_c$  and large superconductor diameter, and a strong reduction of dynamic stability, due to the reduction of the copper's thermal conductivity. Under these circumstances, flux jumps at low fields are inevitable, and the associated heat release could propagate along the conductor in a quench. In magnets, this means that quenches could be initiated in low-field regions at currents well below the designed operating current. We show that by limiting the final reaction duration, it is possible to keep the quench current density above  $J_c$ , thus ensuring flux-jump recovery along the entire magnet load line. For the example studied, keeping the residual resistivity ratio above  $\sim 20$  ensures safe operation. This was achieved for final reactions of 40 h or less, instead of the typical 72–200 h. Surprisingly, the performance penalty was small: a 24 h final reaction reached  $>90\%$  of the highest  $J_c$  obtained. Energy-dispersive spectroscopy in a SEM did not reveal any detectable tin in the copper for stable strands, but in unstable strands as much as 4% Sn was found in the copper between sub-elements, suggesting that the contamination is rather local. The thermal conductivity of the stabilizer should then vary strongly with distance from the sub-element pack to the strand perimeter, complicating stability analyses.

The critical current density  $J_c$  of a superconductor is the primary index of high-field superconducting magnet performance, since the product of coil cross-section and  $J_c$  represents the available number of ampere-turns. Because of this fact, research and development programs push  $J_c$  to ever higher limits. This limit is presently about

3000 A mm<sup>-2</sup> over the conductor area that is not devoted to copper stabilizer for Nb<sub>3</sub>Sn superconductors at 4.2 K and 12 T [1, 2]. Improvement in  $J_c$  has directly led to the achievement of 16 T particle accelerator dipole magnets [3] and magnets capable of supporting nuclear magnetic resonance at  $\sim 1$  GHz [4].

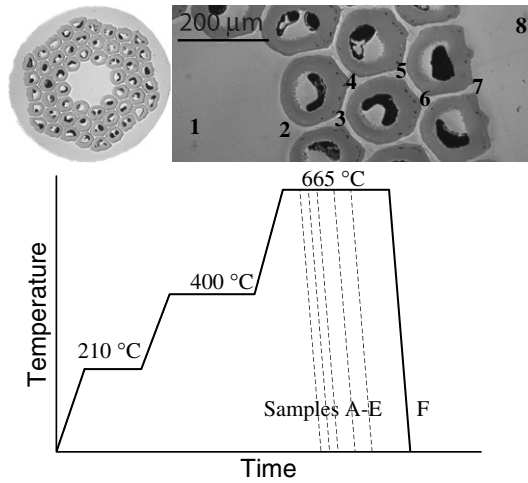


**Figure 1.** Top: image of the conductor cross-section after reaction D. The diameter of the strand in the left image is 0.72 mm. Void space occupies the central region of the sub-elements, which contained tin prior to the reaction. The numbers 1–8 in the magnified view at the right indicate schematically the locations of EDX analyses. Bottom: schematic time–temperature plot showing the different heat treatment schedules applied to the samples. Samples A through F correspond to progressively longer final reaction times.

However, improvement in the critical current density has come at the expense of stability. This has limited progress along the frontier of high-field magnet research because lack of stability in strands caused magnets to quench at fields well below their targets [5, 6]. This is not a new problem [7, 8]. Two primary factors contribute to the lack of stability:

- (1) the effective diameter of the superconducting pathway is often larger than  $\sim 100 \mu\text{m}$ ; and
- (2) the thermal conductivity of the copper stabilizer is reduced by contamination.

Moreover, these factors appear to be innate to the internal-tin conductor design [2, 9], upon which the present state of the art is based. It is thus imperative for continued magnet progress to solve these problems at the strand level.

A generic feature of the internal tin process is a central core of tin that reacts with a surrounding arrangement of alloyed niobium filaments. It is important to realize that the achievement of high non-copper  $J_c$  has come mostly from maximizing the  $\text{Nb}_3\text{Sn}$  area, and to a lesser degree from improving the superconductor itself. This usually means that the  $\text{Nb}_3\text{Sn}$  formation reaction is driven for long periods of time (72–200 h) at moderately high temperatures (650–700 °C). During such reactions the filaments coalesce into a solid mass and substantial reaction of a surrounding Nb diffusion barrier occurs, thus producing the large effective diameter of the  $\text{Nb}_3\text{Sn}$ . In places where the diffusion barrier has thinned, the reaction penetrates through to the copper on the other side, allowing tin to alloy with the copper. Fickett [10] showed that tin is very potent for reducing the electrical conductivity of copper. Thermal conductivity is then reduced according to the Wiedemann–Franz law.

Our experiment suggests that the present heat treatment schedule is excessive from the point of view of strand stability. Reducing the length of the final heat treatment prevents copper

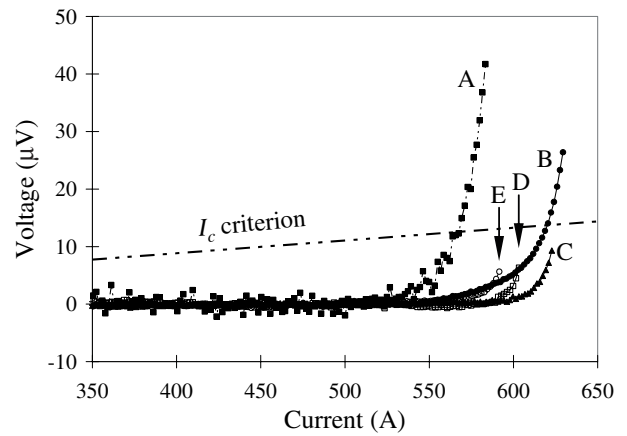


**Figure 2.** Voltage–current transitions acquired at 11.5 T for samples A–E. The resistivity criterion used to determine  $I_c$  is also shown.

**Table 1.** Sample identification, reaction time during final stage at 665 °C, and performance.

Sample	HT time (h)	$J_c$ (A mm <sup>-2</sup> )	$J_s$ (A mm <sup>-2</sup> )	RRR
A	24	2764	4920	130
B	36	2986	3755	47
C	48	2988	2508	13
D	72	2896	1875	5.6
E	96	2857	1772	3.9
F	150	2671	1650	2.9

poisoning, as assessed by the residual resistivity ratio (RRR) of the strands. By applying measurement techniques used three decades ago [11], we then show that this restores enough dynamic stability to the strand to get around the lack of adiabatic stability due to the coalesced filaments. In fact,  $J_c$  can still be  $\sim 90\%$  of the highest value obtained while keeping the RRR high, and this occurs for reactions as short as 24 h. This combination of good performance, dynamic stability, and short reaction time are highly desirable for magnet production.

We applied final reactions of varying length to a restacked-rod process (RRP) strand obtained from Oxford Instruments—Superconducting Technology in Carteret, NJ. A diagram of the different temperature–time schedules and the sample identification is given in figure 1, along with an overview of the strand cross-section. The different experimental samples A through E received final reactions from 24 to 96 h at 665 °C, respectively, and were shorter than that given to control sample F, which received the full 150 h final reaction. This information is summarized in table 1. This scheme was suggested by the manufacturer as a way to prevent tin penetration through the barrier, but the cost to  $J_c$  was not known. The changes in volume during reaction increased the wire diameter from nominally 0.70 mm in the as-received state to 0.72 mm after reaction. The copper stabilizer area fraction was determined by weighing a known length of sample before and after etching the copper completely away.

Critical current  $I_c$  measurements were made using a facility described elsewhere [12]. The transport critical current, determined at a resistivity criterion of  $10^{-14} \Omega \text{ m}$  applied to the measured wire cross-section area, ranged from 500 to 1000 A at fields of  $\sim 8$  up to 11.5 T in a liquid helium bath. It is interesting to note that with increasing reaction times

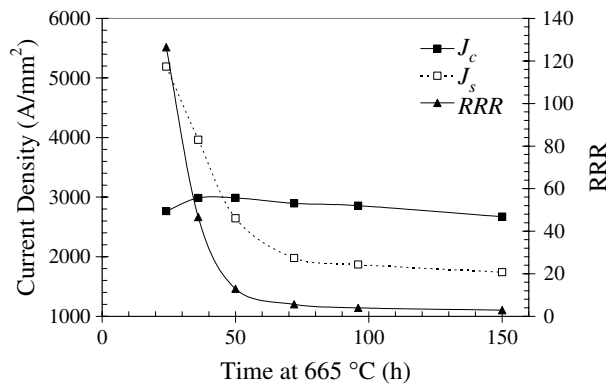


**Figure 3.** Critical current density, magnetic stability threshold current density, and RRR plotted as a function of final reaction time at 665 °C.

the voltage at which quenching occurred decreased, eventually falling below the  $I_c$  criterion. For example, figure 2 shows the voltage–current ( $V$ – $I$ ) curves for the samples at 11.5 T. When the sample quenched before reaching the criterion,  $I_c$  was extrapolated from a power-law fit to the data.

The residual resistance of the wire at 20 K was measured using a separate fixture made out of G-10 fibreglass epoxy. The voltage across a 5 cm section was measured using a current density of 10 A mm<sup>-2</sup> at room temperature and just above the superconducting transition (about 20 K). The RRR was then defined by taking the ratio of the resistance at room temperature and this residual resistance.

The quench behaviour at high field is different in origin than that below about 2 T. At high field, the magnetic energy contained in the critical state is lower than the heat capacity, and quenching occurs due to heat generated by flux motion when the current approaches  $I_c$ . Since the resistivity criterion used here lies well above the detectable onset of voltage due to flux motion and heat generation, it is likely that the generation of local hot spots triggers the quench [13]. At low field, however, the energy contained in the critical state can exceed the heat capacity, a condition that is not adiabatically stable. In this case, small disturbances can trigger massive collapse of the critical state and quenching. However, the particular current and field history of the sample will alter the critical-state profile and, accordingly, the threshold for quenching.

To probe the low-field instability regime, field-sweep measurements were made by applying a constant current and ramping the field over 0–4 T [11]. Details of these measurements were presented in [14]. This is analogous to a dc magnetization measurement with finite transport current. Care was taken to manage the thermal and magnetic history such that a complete critical state was built up prior to applying the current and then making any measurements. The field ramp rate was on the order of 5 mT s<sup>-1</sup>, comparable to the ramp rates of R&D magnets. While monitoring the voltage during the field ramp, it was observed that high current levels produced voltage spikes that did not recover, while lower current levels produced voltage spikes that returned to normal almost instantly. These different behaviours were interpreted as being associated with thermal runaway (quenching) at high currents and thermal recovery at low currents following a flux

**Table 2.** Atomic fraction of tin (%) determined by EDX as a function of location in figure 1 for various samples.

Location	Samples				
	A	C	D	E	F
1	<0.5	<0.5	<0.5	<0.5	0.66
2	<0.5	2.67	1.61	1.32	1.62
3	<0.5	4.26	2.69	3.02	1.72
4	<0.5	2.82	1.93	2.44	2.07
5	<0.5	2.41	1.92	2.17	1.88
6	<0.5	1.73	1.68	1.67	1.61
7	<0.5	0.60	0.59	0.51	0.64
8	<0.5	<0.5	<0.5	<0.5	<0.5

jump. The current density  $J_s$  that divided these regimes was therefore associated with a stability threshold.

A summary of our results is given in figure 3. This figure shows how the RRR,  $J_c$ , and  $J_s$  evolve as a function of the final reaction time. Note that the  $J_c$  values are determined using the wire diameter prior to heat treatment (as is used throughout the literature). The most striking feature is the rapid falloff of both the RRR and  $J_s$  between 24 and 48 h, which is in sharp contrast to the gradual rise and then fall of  $J_c$  with reaction time. Extrapolating between the data points, it appears that the stability current density falls below  $J_c$  at just over 40 h. This means that long reaction times produce magnet strands that are in danger of quenching in low-field zones as the operating current rises toward the critical current. In contrast, below 40 h all regions of a magnet are stable against quenching for all operating currents.

Another central feature of figure 3 is the sharp drop in the RRR that precedes the drop in  $J_s$ . This reflects the well-known fact that the general stability against quenching is related to the purity of the copper [11]. Evidently, for this strand design, which has about 50% copper in the cross-section area, the quench threshold current falls below the critical current when the RRR falls below ~20. According to Fickett [10], even as little as 0.1% Sn can cause this reduction.

It is remarkable that the  $J_c$  extrapolated to<sup>3</sup> 12 T for reaction A, 2764 A mm<sup>-2</sup>, is nearly as high as the maximum value for reaction D, 2988 A mm<sup>-2</sup>. This clearly indicates that  $J_c$  values >90% of the highest values can be obtained without contaminating the copper.

To explore whether detectable levels of tin could be found in the copper stabilizer, strand cross-sections were polished and examined using scanning electron microscopy. Energy-dispersive x-ray spectroscopy (EDX) spectra were acquired for 300 s at the locations labelled 1 through 8 in figure 1, using a 17 kV accelerating voltage. The limit of Sn detection is about 0.5% for these parameters. These measurements are summarized in table 2. Notice that, for samples C to F, these EDX measurements indicate much more tin at locations 2 through 7 than would be necessary to reduce the RRR below the critical value of 20. These samples also exhibited regions where the Nb<sub>3</sub>Sn reaction had penetrated through the barrier, as revealed by backscattered electron imaging.

<sup>3</sup> Since our magnet system is limited to 11.5 T field, we extrapolate from measurements taken at 0.5 T intervals down to about 8 T, depending on strand stability and power supply limitations. Past work, e.g. [12], showed that these extrapolations were within 3% of  $J_c$  values quoted by the manufacturer for identical reaction and testing conditions.

For comparison, sample A did not contain any regions with detectable tin, and also did not exhibit any locations where the diffusion barrier was completely penetrated. The tin content generally diminishes with increasing radius from the strand axis, suggesting a concentration of sources near the inner sub-elements. Reaction F was apparently sufficient to allow a detectable amount of tin to diffuse into the central copper area. Although the separation of sub-elements near regions 2–7 is approximately  $10\text{ }\mu\text{m}$ , we did not detect any trace of Nb in these EDX measurements.

The EDX measurements indicate that gross copper poisoning is locally distributed near the sub-elements (regions 2 through 7) in strands reacted beyond 24 h. Since this should produce a reduction of the thermal conductivity by 1–2 orders of magnitude, it may be valid to approximate these strands as being composed of a single annulus with poor thermal conductivity embedded in copper. In that case, the ratio of perimeter  $P$  to area  $A$  of the annulus determines whether heat can be transported radially outward to the coolant bath or propagates along the strand in a quench. However, since this is a factor of  $\sim 10$  lower than  $P/A$  for an individual sub-element embedded in clean copper, as for strand A, the change of length scale alone could drive the onset of instability.

To confirm that these changes were indeed dynamic and not adiabatic in nature, dc magnetization measurements were compared for the same field cycle and field steps using a commercial SQUID magnetometer. This revealed no striking differences in the flux-jump behaviour between samples A–F, after normalizing for changes in the amount of  $\text{Nb}_3\text{Sn}$  area. Since the magnetometer probes the loss of induced current in small ( $\sim 6\text{ mm}$  long) samples, it is sensitive to the adiabatic conditions only and cannot discern the momentary temperature rise due to the energy released during a flux jump. Based on these measurements, it can be concluded that a similar lack of adiabatic stability existed for the entire range of samples. Any differences in critical current stability, therefore, must come from differences in dynamic stability. The magnetic measurements are consistent with having the same length scale for the magnetization current loop, which is set by the sub-element diameter because the diffusion barrier is partially reacted to form superconductor in all cases.

Thus, the entirety of the data lead us to conclude that a primary cause of strand instabilities in high-field  $\text{Nb}_3\text{Sn}$  magnets is over-reaction and loss of thermal conductivity in the copper. We base this conclusion on the steep drop in the value of the RRR that precedes the drop in quench threshold current as a function of reaction time. For the particular strand examined, the quench threshold current fell below the critical

current of the strand for reactions longer than about 40 h. This crossover between quench and critical currents means that magnets made with over-reacted strands may not recover from quenches initiated in their low-field regions. Such quenches are inevitable due to the lack of adiabatic stability inherent to high- $J_c$  internal-tin strand designs. By maintaining high thermal conductivity of the copper stabilizer, the heat generated by flux jumps can be transferred to the coolant bath, enabling magnet operation.

## Acknowledgments

We would like to acknowledge discussions with E Barzi, A Zlobin, V Kishikin, D Dietderich, L Goodrich, J Parrell, and S Hong. This work was supported by the US Department of Energy under Contract No. DE-AC02-98CH10886.

## References

- [1] Dietderich D R 2004 (Lawrence Berkeley National Laboratory) private communication
- [2] Parrell J A, Field M B, Zhang Y and Hong S 2004 *Adv. Cryog. Eng.* **50** 369
- [3] Lietzke A F *et al* 2004 *IEEE Trans. Appl. Supercond.* **14** 345
- [4] Wada H and Kiyoshi T 2002 *IEEE Trans. Appl. Supercond.* **12** 715
- Hashi K *et al* 2002 *J. Magn. Reson.* **156** 318
- Markiewicz W D *et al* 2000 *IEEE Trans. Appl. Supercond.* **10** 728
- [5] Barzi E *Fermi National Accelerator Laboratory Internal Document* TD-04-024 available at [http://www-td.fnal.gov/info/td\\_library.html](http://www-td.fnal.gov/info/td_library.html)
- [6] See for instance *Workshop on Instabilities in  $\text{Nb}_3\text{Sn}$  Strands, Cables, and Magnets (Fermi National Accelerator Laboratory, April 2004)* (summary) available at <http://tdserver1.fnal.gov/nb3sn/workshop/>
- [7] King C G *et al* 1997 *IEEE Trans. Appl. Supercond.* **7** 1524
- [8] Wilson M N 1983 *Superconducting Magnets* (Oxford: Clarendon) especially chapters 5–9
- [9] For a review see Miyazaki T, Hase T and Miyatake T 2003 *Handbook of Superconducting Materials* ed D A Cardwell and D S Ginley (Bristol: Institute of Physics Publishing) chapter B3.3.3 (Processing of Low  $T_c$  Conductors: the Compound  $\text{Nb}_3\text{Sn}$ )
- [10] Fickett F R 1982 *Cryogenics* **35** 135
- [11] Wilson M N and Walters C R 1970 *J. Phys. D: Appl. Phys.* **13** 1547
- [12] Soika R, Cooley L D, Ghosh A K and Werner A 2004 *Adv. Cryog. Eng.* **50** 67
- [13] Gurevich A V I and Mints R G 1981 *J. Phys. D: Appl. Phys.* **14** 1129
- [14] Details of these measurements were presented by Ghosh A K, Cooley L D and Moodenbaugh A M 2005 *Applied Superconductivity Conf. (Jacksonville, FL)* paper 2MR-03; *IEEE Trans. Appl. Supercond.* **15** at press